www.czasopisma.pan.pl PAN POLSKA AKADEMIA NAUK www.journals.pan.pl

A R C H I V E S O F M E T A L L U R G Y A N D M A T E R I A L S

Volume 59 2014 Issue 2

DOI: 10.2478/amm-2014-0105

Z. RDZAWSKI*,**, W. GŁUCHOWSKI*, J. STOBRAWA*,**, J. SOBOTA*

EFFECT OF RARE-EARTH METALS ADDITION ON MICROSTRUCTURE AND PROPERTIES OF SELECTED COPPER ALLOYS

WPŁYW DODATKU METALI ZIEM RZADKICH NA MIKROSTRUKTURĘ I WŁAŚCIWOŚCI WYBRANEGO STOPÓW MIEDZI

Effect of addition of rare earth metals on microstructure and properties of copper alloys after casting, after cold working and after heat treatment was studies in this paper. Methodology consisted of microstructure investigations by optical microscopy and scanning electron microscopy. In addition, distribution of alloying elements and electron backscattered diffraction results (EBSD) were presented. The mechanical properties of a wire after tension test and after hardness measurements were described. Electrical conductivity test was performed using Foerster Sigmatest and Thomson bridge. Analysis of the microstructure and mechanical properties of investigated alloys after casting and after metal working showed possibility to produce materials with preferred set of functional properties.

Keywords: copper and silver alloys, rare earth metals, microstructure, mechanical properties, electrical conductivity

W pracy badano wpływ dodatku metali ziem rzadkich na mikrostrukturę i właściwości użytkowe stopów miedzi w stanie po odlewaniu, po przeróbce plastycznej na zimno i po obróbce cieplnej. Metodyka badawcza obejmowała obserwacje mikrostruktury z wykorzystaniem mikroskopu optycznego i elektronowego mikroskopu skaningowego. Dodatkowo dla stopów przeprowadzono badanie rozmieszczenia składników stopowych na powierzchni badanego materiału oraz badanie EBSD. Właściwości mechaniczne drutu opisano w oparciu o wyniki próby zrywania i pomiaru twardości HV. Badanie konduktywności elektrycznej wykonano za pomocą Sigmatestu firmy Foerster oraz mostku Thomsona. Analiza mikrostruktury i właściwości mechanicznych po przeprowadzonych badaniach na stopach odlewanych i po przeróbce plastycznej, wykazała że możliwe jest wytworzenie materiałów cechujących się korzystnym zestawem własności użytkowych.

1. Introduction

Rare earth metals are among the materials becoming more widely used in industrial practice. Application of rare earth metals increases with development of industries which manufacture advanced products, such as hybrid cars, batteries, mobile phones, flat screens and displays (LED, LCD, plasma), plasma TV sets, energy saving light bulbs, generators of wind power plants, industrial engines, MRI (Magnetic resonance imaging) machines, iPods and computer hard drives [1-3].

Application of rare earth metals has significant influence on development of environmentally friendly technologies and on limitation of greenhouse gases emission. Even addition of some per mille of the elements to the material may result in its higher strength or in generation of strong magnetic field, therefore rare earth metals are necessary in all advanced technologies. Additional advantage of rare earth metals is their non-toxicity [4-6].

The most often used alloying additions (in the amount significantly lower than 1 wt %) are cerium and mischmetal, i.e. product of refining of rare earth metals concentrates without separation of individual elements.

Small addition of lanthanides may bring better anticorrosion properties in metals and alloys protected on the surface by oxide layer. It is also confirmed that at least cerium acts as a grain refining agent in some steels, aluminum alloys and magnesium alloys, increasing their mechanical properties and resistance to fatigue. The main advantage resulting from application of rare earth metals addition to non-ferrous metals alloys can be seen in deoxidization and purification of metal bath during melting, refinement of cast metal microstructure and stabilization of microstructure and mechanical properties at elevated temperature, as well as in additional increase of alloy strength thanks to the presence of small particles of the second phase [7-9].

The available literature provides only few articles on studies into Cu-Ag alloys with addition of rare earth metals. There is a is widely known possibility to improve strength of Cu-Ag alloy by application of a third component (e.g. Nb, Cr and Zr).

The conducted so far studies show that addition of rare earth metals to pure copper may result in removal of harmful elements, such as oxygen, sulfur, hydrogen and other impurities (e.g. Bi, Sn, Pb), in this way improving microstructure of

* INSTITUTE OF NON-FERROUS METALS, UL. SOWIŃSKIEGO 5, 44-100 GLIWICE, POLAND

** INSITUTE OF ENGINEERING MATERIALS AND BIOMATERIALS, SILESIAN UNIVERSITY OF TECHNOLOGY, 18A KONARSKIEGO STR., 44-100 GLIWICE, POLAND

copper after casting [10-15]. Addition of Ce to pure copper facilitates microstructure refinement, thus improving mechanical properties [16].

Addition of rare earth metals to copper promotes generation of fine-grained microstructure as observed in steels and aluminum and magnesium alloys where rare earth metals play a role of crystal nuclei. At the same time, because of their strong chemical affinity to oxygen and other elements, the rare earth metals neutralize disadvantageous influence of copper matrix impurities which leads to generation of high electrical conductivity of those alloys.

This study presents results of investigations into microstructure and functional properties of new copper alloys with addition of rare earth metals. Such materials can be applied in production of electric transformers, strong electromagnets for metal transportation and in equipment for plastic deformation by magnetic field.

2. Methodology, material for studies

The following alloys were used in the studies:

- Cu-Ag15%, (marked as Cu-Ag)
- Cu-Ag15% + 0,5% mischmetal (marked as Cu-Ag-Mm)

The alloys were produced by melting and casting in a vacuum induction furnace. Base components and alloying additions were introduced into a graphite crucible before melting. Metal in the crucible was heated up to the temperature over 1,100°C, and then the temperature in furnace was reduced for degassing operation. The alloy was cast into a graphite ingot mould of round cross section of diameter about 20 mm and slowly cooled down in the air. After cooling down the ingot top was cut off and a layer of impurities from side surfaces of the ingot was removed by machining process.

Ingots made of Cu-Ag, Cu-Ag-Mm were rolled down with grooved rolls into a 6.4 mm square wire and then to diameter of 1.4 mm, and next it was drawn to diameter of 0.5 mm.

After that heat treatment of the Cu-Ag and Cu-Ag-Mm wires was performed in electric resistance furnace in protective gas. The material was annealed in temperature of 200°C and 500°C for 3 and 7 hours.

After casting, metal working and heat treatment microstructure of the material was examined (in the cast material additionally macrostructure was examined) with Olimpus GX71 optical microscope and Zeiss Leo Gemini 1525 electron scanning microscope equipped with Roenteck EDS chemical composition microanalyser. Also studies into distribution of alloy components on the surface of the material were performed by WDS technique as well as EBSD examination with Jeol JXA- 8230 microanalyser.

Mechanical properties of the wire were examined by tensile test in Instron testing machine and HV hardness was determined. Electrical conductivity was determined with Foerster Sigmatest and Thomson bridge.

3. Results and discussion

3.1. Macro- and microstructure after casting

In macrostructure of a Cu-Ag ingot without rare earth metals some areas of chill, columnar and equiaxed crystals were present. Addition of mischmetal to Cu-Ag alloy resulted in refinement of macrostructure. The macrostructure of Cu-Ag-Mm alloy was fine-grained, without areas of chill, columnar and equiaxed crystals, characteristic for casting by batch method.

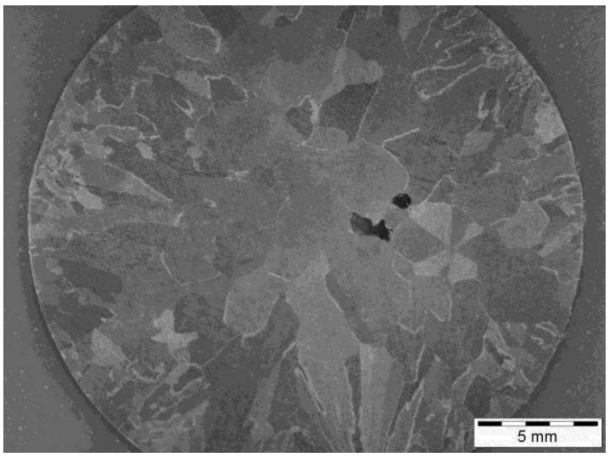

Fig. 1. Sample macrostructure of Cu-Ag alloy ingot

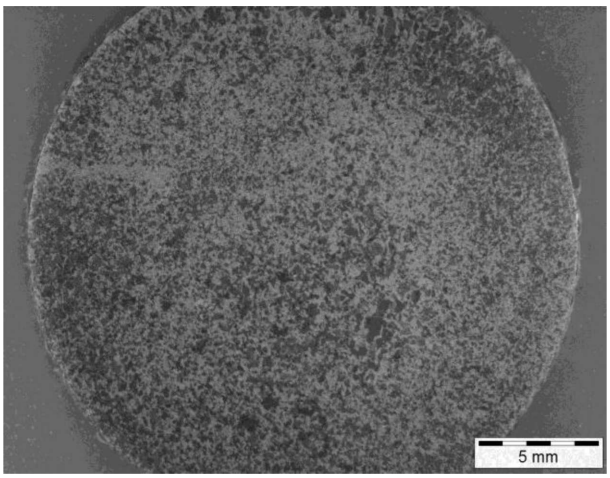

Fig. 2. Sample macrostructure of Cu-Ag-Mm alloy ingot

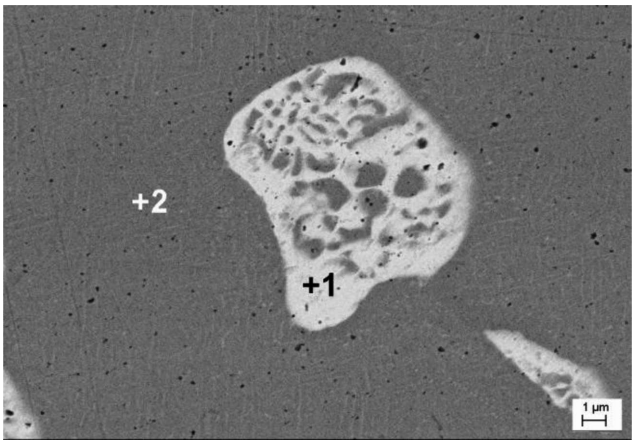

Fig. 3. Microstructure of Cu-Ag alloy with results of EDS microanalysis in microsections: 1: Ag=93.27%, Cu=6.73%, 2: Ag=5.70%, Cu=94.30%; polished section, SEM

Rare earth metals present limited solubility in Cu and Ag, therefore enrichment of atoms of rare earth metals, which is forming along the liquid-solid interface surface, can block the liquid-solid transfer and reduce phase crystallization rate

or growth of α grains. Addition of rare earth metals facilitates also formation of eutectic.

Figures 3-4 present sample images of microstructure observed by scanning electron microscopy, supplemented with results of chemical composition analysis in microsections (EDS).

Silver-rich phase in Cu-Ag alloys was observed in boundaries of grains of Cu-rich matrix. In the alloys with mischmetal addition rare earth metals were usually observed in a form of oxides also in boundaries of grains of Cu-rich matrix.

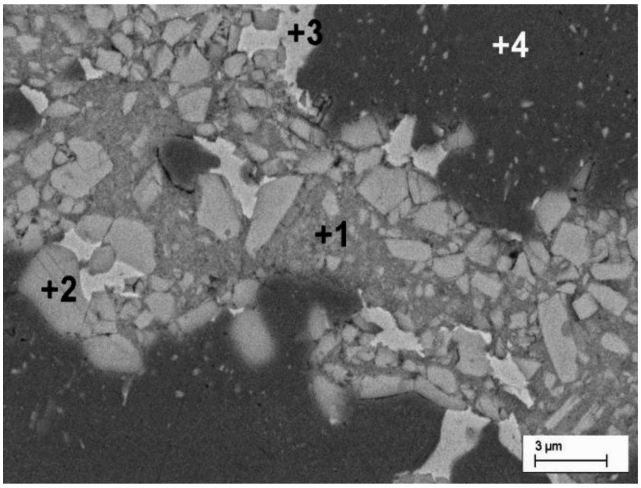

Fig. 4. Microstructure of Cu-Ag-Mm alloy with results of EDS microanalysis in microsections: 1: O=29.18%, La=25.13%, Ce=42.32%, Cu=3.37%; 2: O=34.72%, La=22.29%, Ce=40.26%, Cu=2.74%; 3: Ag=94.98%, Cu=5.02%; 4: Ag=4.97%, Cu=95.03%; polished section, SEM

3.2. Microstructure after cold metal working

Investigations into microstructure and mechanical properties were conducted with cast alloys and showed a possibility for their further cold metal working in production of materials with advantageous functional properties.

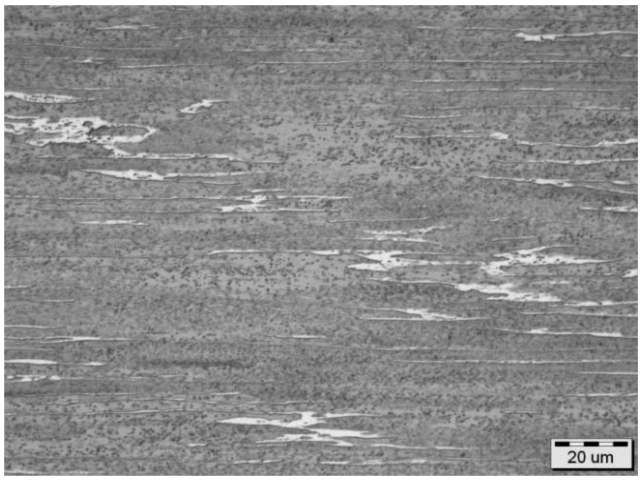

Fig. 5. Microstructure of Cu-Ag wire of diameter 6,4 mm, longitudinal section

Cu-Ag, Cu-Ag-Mm alloys were processed by cold metal working, covering rolling and drawing.

Ingots were rolled down with profile rolls into a 1.4 mm square wire and next the wire was drawn down to diameter of 0,5 mm.

Fig. 5-6 present microstructure of Cu-Ag, Cu-Ag-Mm wires of diameter 6,4 mm on the section longitudinal to the rolling direction, and Fig. 7-8 show microstructure of Cu-Ag, Cu-Ag-Mm wires of diameter 0,50 mm after cold metal working.

No differences between microstructure of Cu-Ag and Cu-Ag-Mm wire were observed. In Cu-Ag and Cu-Ag-Mm alloys of diameter 6,4 mm short bands of Ag-rich phase were visible. Fibers were not continuous along the whole wire length and the distance between consecutive bands of fibers were in the range 1-10μm.

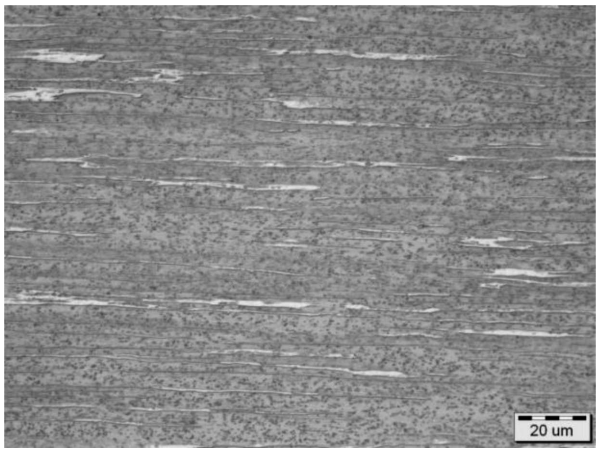

Fig. 6. Microstructure of Cu-Ag-Mm wire of diameter 6,4 mm, longitudinal section

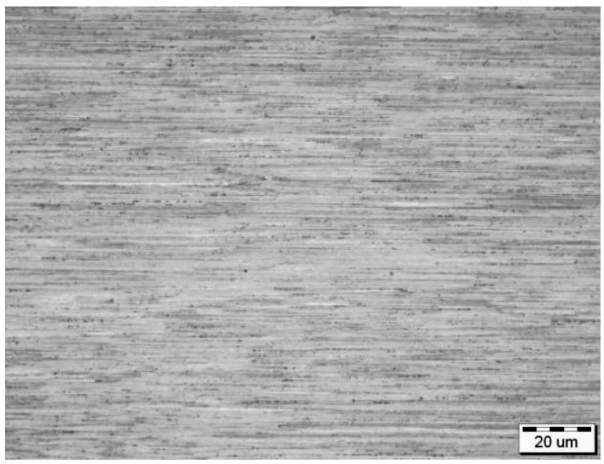

Fig. 7. Microstructure of Cu-Ag wire of diameter 0,50 mm, longitudinal section

Fibers in Cu-Ag and Cu-Ag-Mm wire of diameter 0,50 mm were evenly distributed along the whole length of alloy, following the direction of rolling and drawing.

Figures 9-10 present images of microstructure observed by scanning electron microscopy, supplemented with results of chemical composition analysis in microsections (EDS).

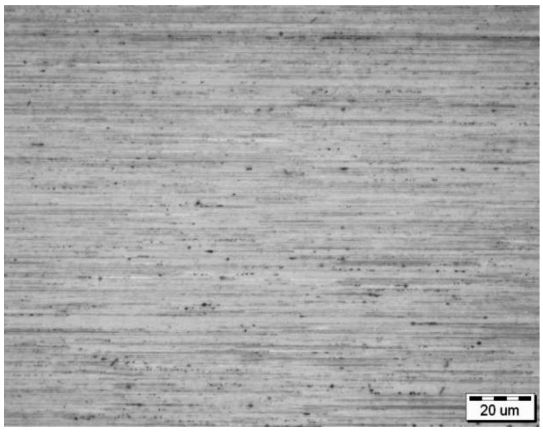

Fig. 8. Microstructure of Cu-Ag-Mm wire of diameter 0,50 mm, longitudinal section

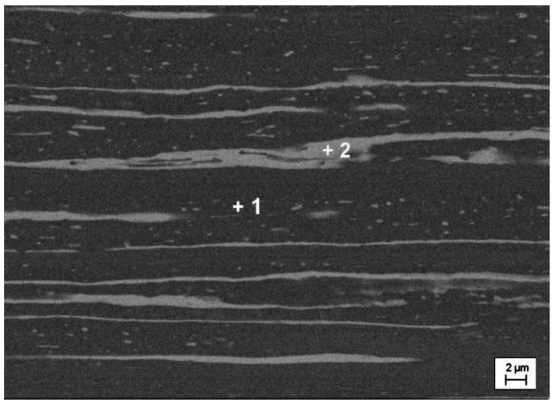

Fig. 9. Microstructure of Cu-Ag wire with results of EDS microanalysis in microsections: 1:Cu 91,5%, Ag 8,5%, 2:Cu 14,7%, Ag 85,3%; longitudinal section

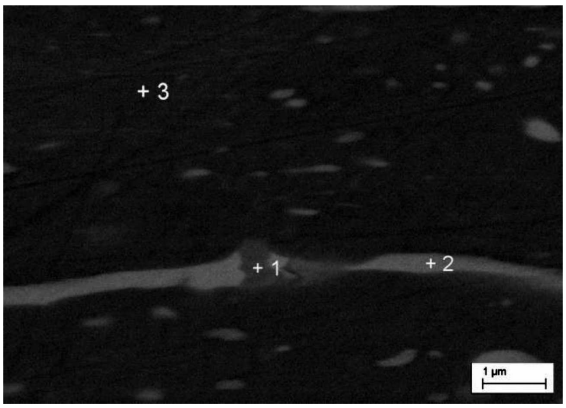

Fig. 10. Microstructure of Cu-Ag-Mm wire with results of EDS microanalysis in microsections: 1: Cu 50,3%, Ag 31,9%, O 11,0%, Ce 4,7%, La 2,1%; 2: Cu 24,5%, Ag 73,% 3: Cu 93,5%, Ag 6,5%; longitudinal section

The rich in silver phase in Cu-Ag alloys was in a form of bands in the matrix of the Cu-rich phase. In the Cu-Ag alloy with mischmetal addition rare earth metals were usually observed in a form of oxides in the area of Ag-rich phase. Cold plastic deformation resulted in refinement of microstructure in which bands of silver-rich phase alternate with bands of copper-rich phase.

The arrangement of alloy components observed by WDS technique in samples after metal working is presented in Fig. 11 and 12.

Chemical analysis on the surface of Cu-Ag alloy structure revealed presence of: Cu 85.3% , Ag 14.7% (wt %). In Cu-Ag-Mm alloy the surface composition was as follows: Cu – 85.29%, Ag – 14.63%, Ce – 0.08% (wt %).

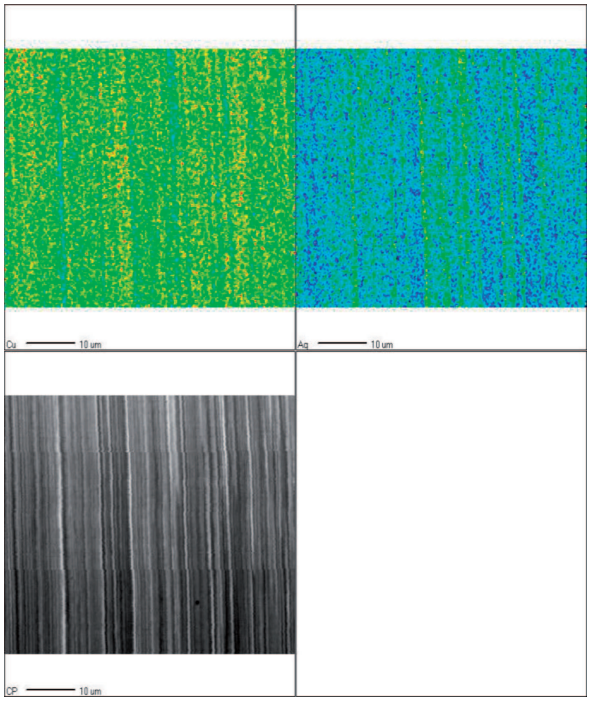

Fig. 11. Maps of element distribution (WDS) in Cu-Ag alloy. Section lengthwise to extrusion direction, magn. 2000x

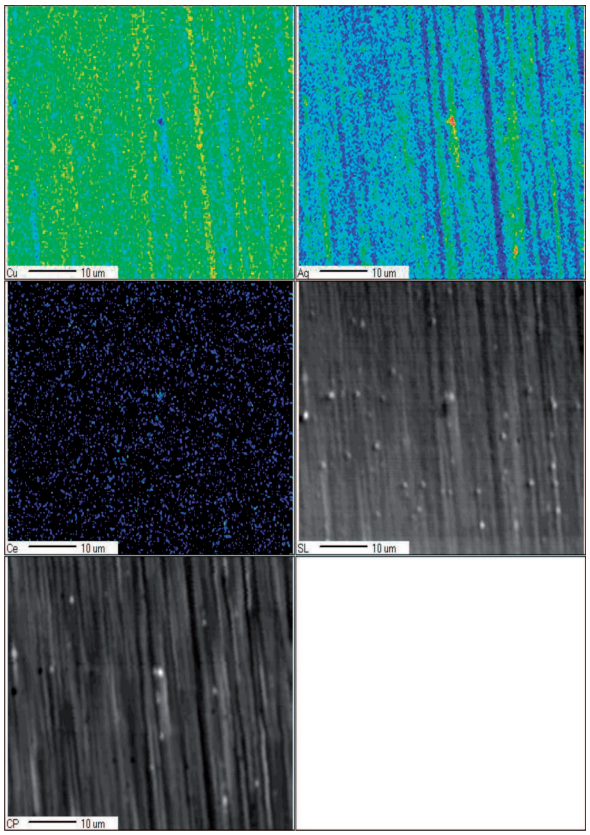

Fig. 12. Maps of element distribution (WDS) in the area of increased Ce and La concentration in Cu-Ag-Mm alloy. Section lengthwise to extrusion direction, magn. 2000x

3.3. Mechanical and electrical properties after metal working

For Cu-Ag, Cu-Ag-Mm alloys subjected to metal working by multiple rolling and drawing from diameter of 6,4 mm to 0,5 mm, a work-hardening curve was determined in tensile test. Ultimate tensile strength of Cu-Ag wire of diameter 0,5 mm increased to 1120,5 MPa. Yield point of the wire of diameter 0,5 mm increased over twofold when compared to the wire of diameter 6,4 mm.

In Cu-Ag-Mm wire of diameter 0,5 mm the tensile strength increased to 986,5 MPa (about 45% when compared to the wire of diameter 6,4 mm).

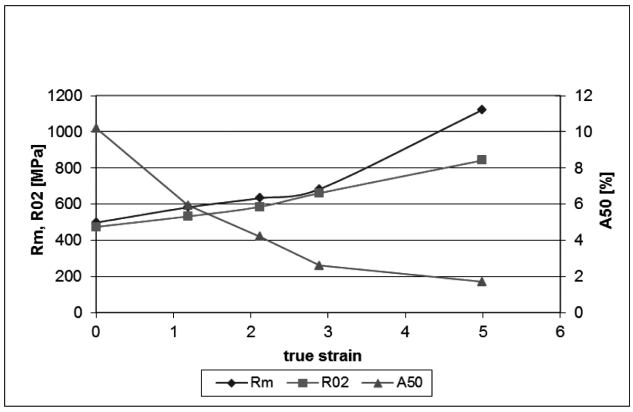

Fig. 13. Work-hardening curves of Cu-Ag wire reduced from 6,4 mm diameter to 0,5 mm

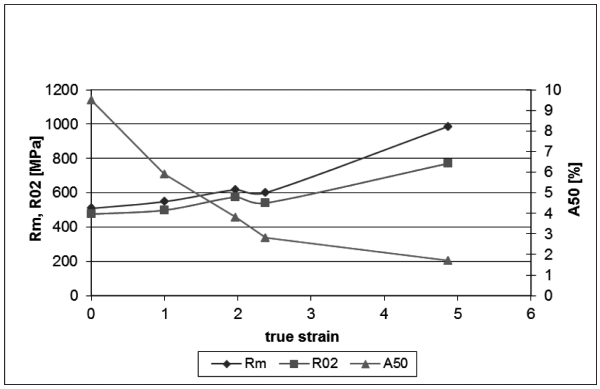

Fig. 14. Work-hardening curves of Cu-Ag-Mm wire reduced from 6,4 mm diameter to 0,5 mm

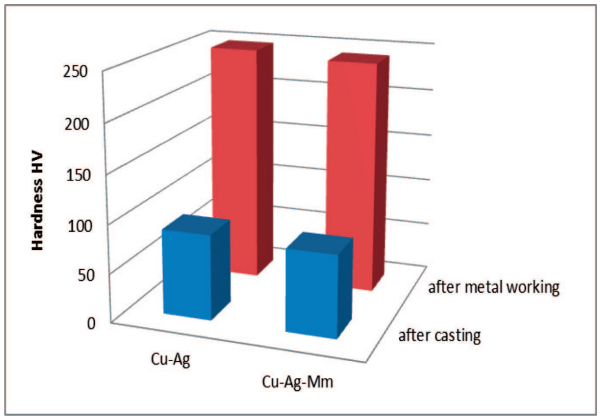

Fig. 15. Hardness of alloys after casting and metal working

Results of alloy hardness examination after casting and metal working are presented in Figure 15. Hardness of Cu-Ag and Cu-Ag-Mm alloys after metal working increased three times when compared to the hardness after casting.

Figure 16 presents results of electrical conductivity examination after casting and after metal working. The highest electrical conductivity was reached in the alloy after metal working with mischmetal addition.

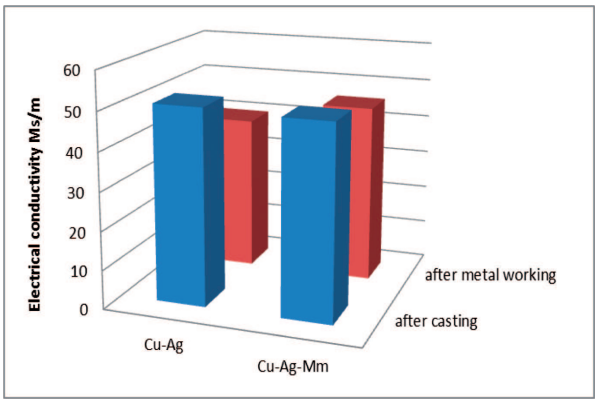

Fig. 16. Electrical conductivity after casting and metal working

3.4. Microstructure after heat treatment

Four variants of heat treatment (200°C/3h, 200°C/7h, 500°C/3h, 500°C/7h) were used with Cu-Ag and Cu-Ag-Mm wire of diameter 0,5 mm. Since no significant differences were observed in the examined microstructure with changes of heat treatment parameters the microstructure of Cu-Ag and Cu-Ag-Mm wire is presented for selected variants of heat treatment only.

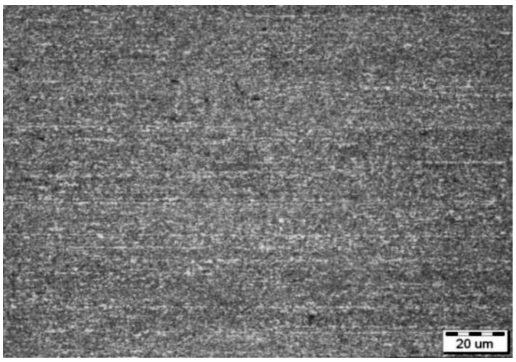

Fig. 17. Microstructure of Cu-Ag wire of diameter 0,5 mm after heat treatment in 200°C/7h, longitudinal section

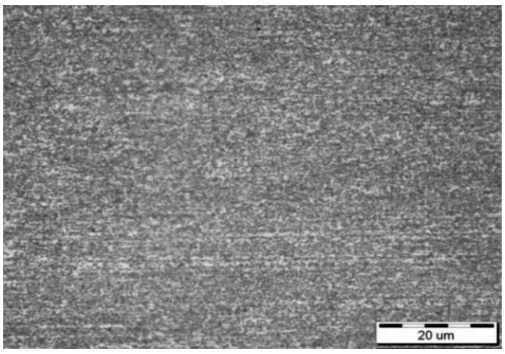

Fig. 18. Microstructure of Cu-Ag wire of diameter 0,5 mm after heat treatment in 500°C/7h, longitudinal section

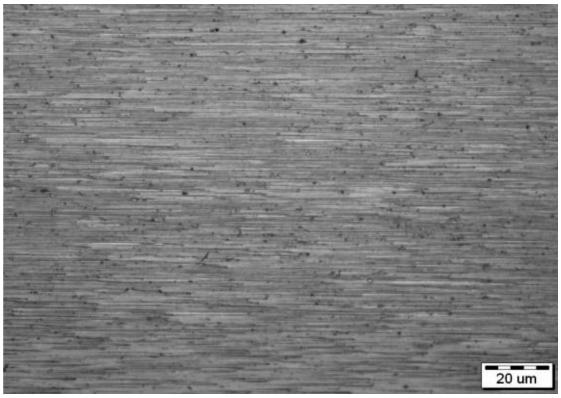

Fig. 19. Microstructure of Cu-Ag-Mm wire of diameter 0,5 mm after heat treatment in 200°C/7h, longitudinal section

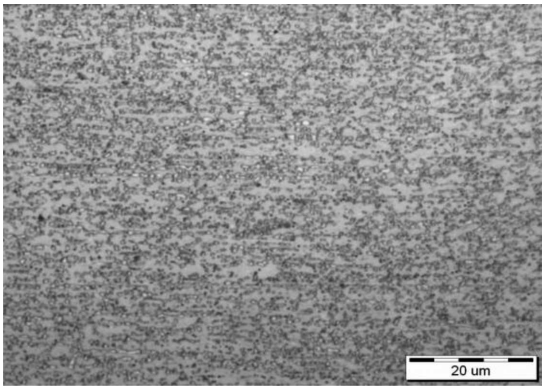

Fig. 20. Microstructure of Cu-Ag-Mm wire of diameter 0,5 mm after heat treatment in 500°C/7h, longitudinal section

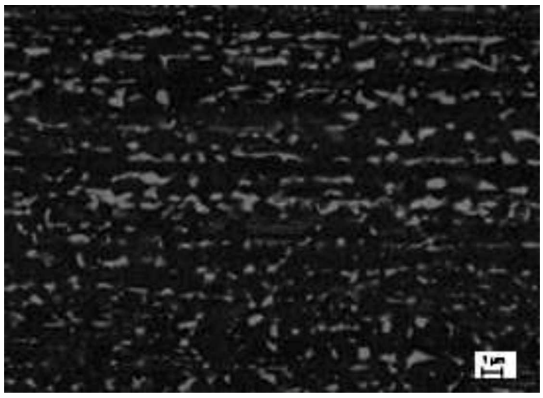

Fig. 21. Microstructure of Cu-Ag wire of diameter 0,5 mm after heat treatment in 200°C/7h, longitudinal section

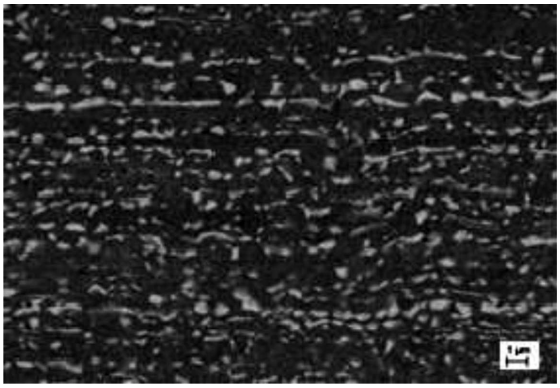

Fig. 22. Microstructure of Cu-Ag wire of diameter 0,5 mm after heat treatment in 500°C/7h, longitudinal section

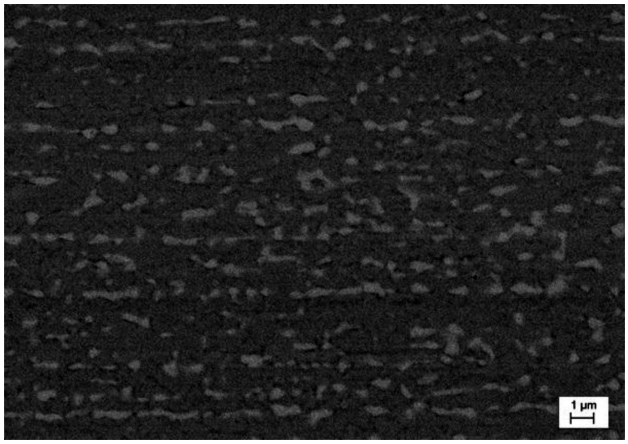

Fig. 23. Microstructure of Cu-Ag-Mm wire of diameter 0,5 mm after heat treatment in 200°C/7h, longitudinal section

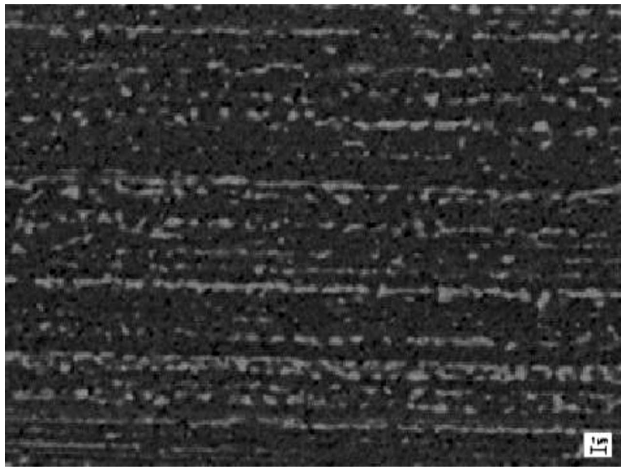

Fig. 24. Microstructure of Cu-Ag-Mm wire of diameter 0,5 mm after heat treatment in 500°C/7h, longitudinal section

Results of studies into microstructure of Cu-Ag and Cu-Ag-Mm wire after strain and heat treatment (in 500°C for 7h) by EBSD technique are presented in Fig. 25-30. The average grain diameter in Cu-Ag material was 1,6μm, and the maximum diameter was below 6μm. No twin boundaries were observed. High-angle boundaries (over 15°) represented 83% of the total amount of grain boundaries.

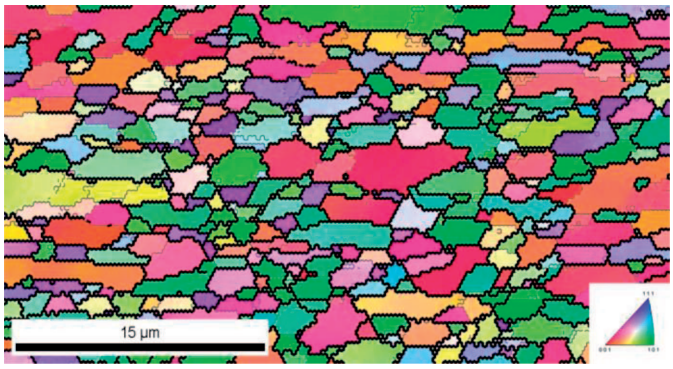

Fig. 25. Map of grains and map of crystallographic orientation distribution in Cu-Ag all

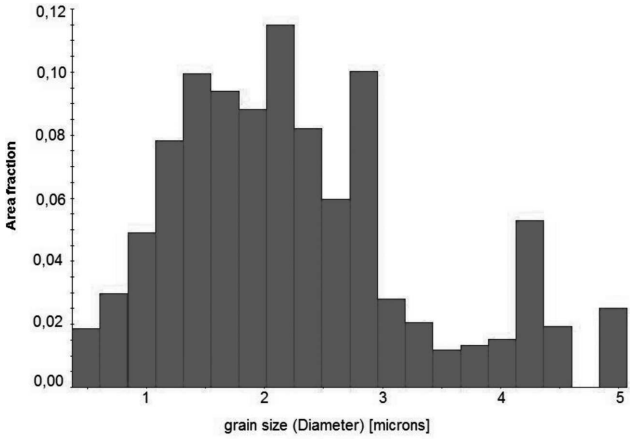

Fig. 26. Grain size distribution in Cu-Ag alloy

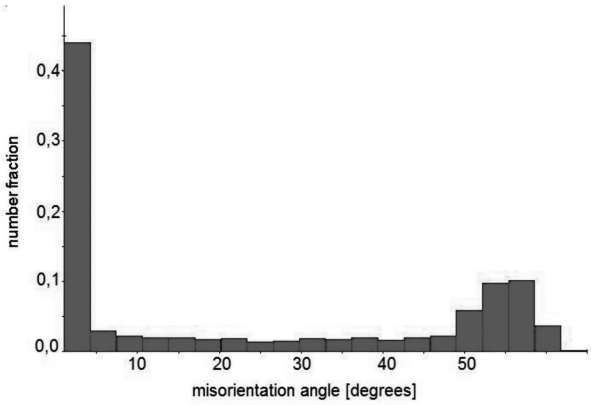

Fig. 27. Misorientation angle distribution in Cu-Ag alloy

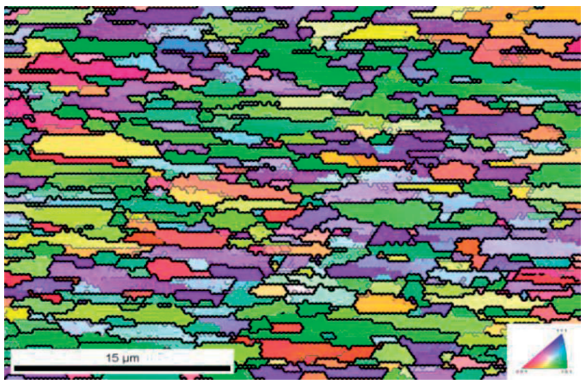

Fig. 28. Map of grains and map of crystallographic orientation distribution in Cu-Ag-Mm alloy

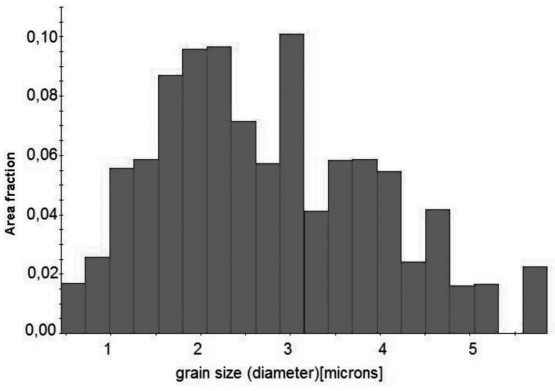

Fig. 29. Grain size distribution in Cu-Ag-Mm alloy

The average grain diameter in Cu-Ag-Mm material was 1,3μm, while the maximum diameter was below 5μm. No twin boundaries were observed. High-angle boundaries (over 15°) represented 90% of the total amount of grain boundaries.

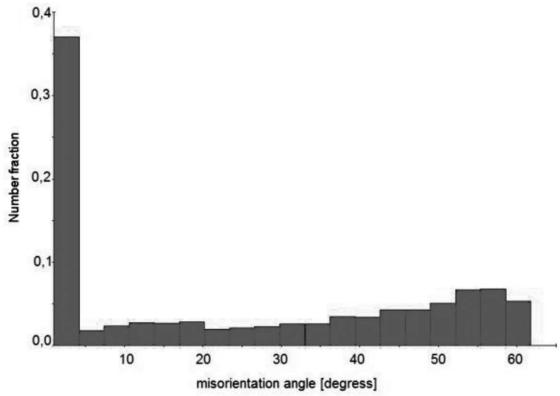

Fig. 30. Misorientation angle distribution in Cu-Ag-Mm alloy

3.5. Mechanical and electrical properties after casting, straining and heat treatment

Results of alloy hardness examination after casting, after metal working and after heat treatment are presented in Figure 31.

Hardness of Cu-Ag and Cu-Ag-Mm alloys after heat treatment decreased below 150 HV. Higher hardness after heat treatment was reached in Cu-Ag-Mm alloy.

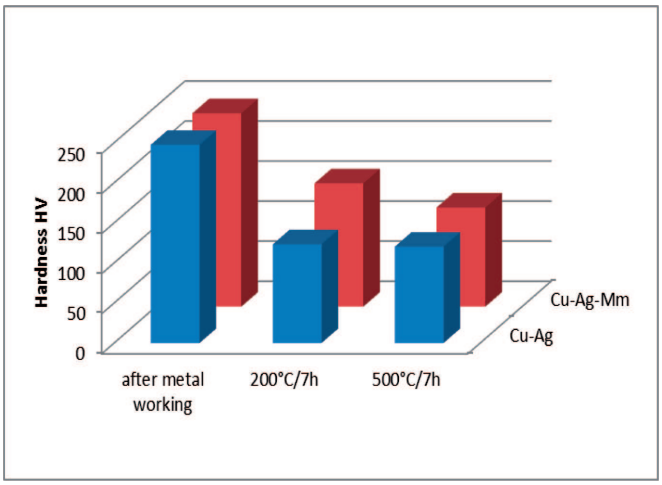

Fig. 31. Hardness of alloys after casting, metal working and annealing

Figure 32 presents results of electrical conductivity examination after casting, after metal working and heat treatment. The highest, comparable in Cu-Ag alloy and alloy with mischmetal addition, electrical conductivity was reached after annealing in 500°C for 7 hours.

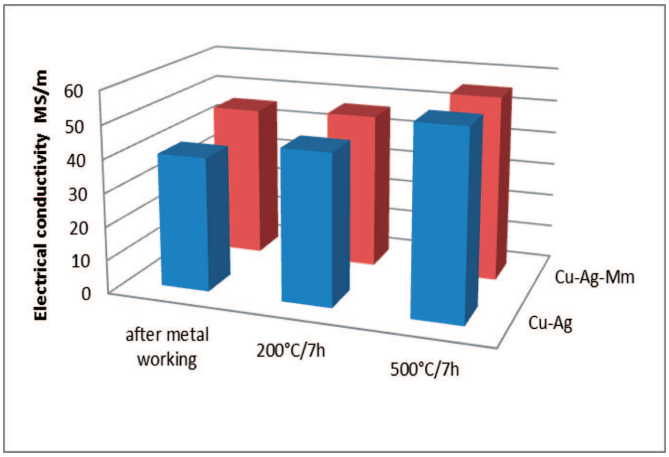

Fig. 32. Electrical conductivity of alloys after casting, after metal working and heat treatment

After straining and heat treatment the examined materials were tensile tested. Both in Cu-Ag and Cu-Ag-Mm alloy the highest tensile strength and proof stress were reached with annealing temperature of 200°C and time of 3 hours. Decrease of tensile strength and proof stress with time or temperature increase was observed. The test results are presented in Table 1.

TABLE 1

Tensile strength, proof stress and elongation of Cu-Ag and Cu-Ag-Mm alloys after casting, straining and heat treatment

material	annealing temp.	annealing time	Rm [MPa]	R0,2 [MPa]	A 50%
Cu-Ag	200°C	3 h	1087,4	871,8	2,5
		7h	1086,4	804,5	2,3
	500°C	3h	371,6	286,9	8,3
		7h	337,5	252,4	16,0
Cu-Ag-Mm	200°C	3h	976,5	762,5	2,4
		7h	969,0	754,2	2,1
	500°C	3h	384,9	281,9	10,5
		7h	344,2	188,4	10,3

4. Summary

Addition of mischmetal to Cu-Ag alloy resulted in microstructure refinement which then brought higher mechanical properties. Additionally increase of electrical conductivity of the material after straining was observed. Cold metal working of Cu-Ag and Cu-Ag-Mm alloys resulted in significant hardness increase with small decrease of electrical conductivity.

Annealing of Cu-Ag and Cu-Ag-Mm wires of diameter 0,5 mm in temperature of 200°C brought insignificant decrease of mechanical properties and proof stress, while annealing in 500°C resulted in their significant drop. In the result of heat treatment electrical conductivity of the examined alloys increased while their hardness decreased.

Analysis of microstructure and mechanical properties of the alloys after casting, after metal working and heat treatment showed possibility to produce materials of advantageous functional properties. Depending on the application of the examined material the advantageous functional properties can be reached after cold metal working already, without application of a subsequent annealing process.

Acknowledgements

The study was supported by Wrocław Research Centre EIT+ within the project "The Application of Nanotechnology in Advanced Materials" NanoMat (POIG.01.01.02-02-002/08) financed by the European Regional Development Fund (Innovative Economy Operational Programme, 1.1.2).

REFERENCES

[1] C. Mingzhen, J. Yunjing, J. Chinese Rare Earth Soc. **5**, 011 (1987).
[2] E. Hanczakowska, P. Hanczakowski, Wiad. Zootechn **48**, 15 (2010).
[3] D. Sierakowska, Trend **10**, 10 (2008).
[4] T. Pieczonka, rozdz.21, Inżynieria metali i ich stopów, Wydawnictwo AGH, Kraków 2012, 627-632.
[5] K. Ozaki, AIST Today, Summer 29, 4-5 (2008).
[6] C. Hurst, Institute for the Analysis of Global Security, report,March 2010.
[7] W. Głuchowski, J. Sobota, Rudy Metale **10**, 527 (2011).
[8] W. Głuchowski, Z. Rdzawski, J. Achiev. Mater. Manuf. Eng. **30**, 2, 129-134, October 2008.
[9] W. Głuchowski, Z. Rdzawski, J. Stobrawa, Konferencja sprawozdawcza komitetu Metalurgii PAN Metalurgia, Krynica-Zdrój (2010).
[10] D.H. Xiao, J.N. Wang, D.Y. Ding, J. Alloys Compd. **352**, 84 (2003).
[11] Y. Lu, Q.D. Wang, X.Q. Zeng, Mater. Sci. Eng. A **278**, 66 (2000).
[12] N.C. Si, Y. Guo, G.Q. Li, Chin. J. Nonferrous Met. **16**, 606 (2006).
[13] M.F. Jiang, Y.K. Yao, C.J. Liu, J. Rare Earths **21**, 194 (2003).
[14] X.W. Zeng, J. Rare Earths **23**, 434 (2005).
[15] C.Y. Yu, L.M. Wang, J.H. Liu, J. Rare Earths **23**, 493 (2005).
[16] Z. Zhang, G. Lin, S. Zhang, J. Zhou, Mater. Sci. Eng. A **457**, 313 (2007).

Received: 10 September 2013.